Received: 30 September 2016 | Revised: 26 June 2017 | Accepted: 10 October 2017

DOI: 10.1002/fam.2485

WILEY

SPECIAL ISSUE PAPER

Modeling of fire exposure in facade fire testing

J. Anderson[1] | L. Boström[1] | R. Jansson McNamee[2] | B. Milovanović[3]

[1] RISE Safety and Transport, Fire Research, Brinellgatan 4, Box 857, S-501 15 Borås, Sweden

[2] Brandskyddslaget AB, Långholmsgatan 27 Box 9196, 102 73 Stockholm, Sweden

[3] Faculty of Civil Engineering, Department of Materials, University of Zagreb, Kaciceva 26, 10000 Zagreb, Croatia

Correspondence
1RISE Safety and Transport, Fire Research, Brinellgatan 4, Box 857, S-501 15 Borås, Sweden.
Email: johan.anderson.br@sp.se

Funding information
Swedish Fire Research Board (Brandforsk), Grant/Award Number: BF-14-0011

Summary

In this paper, a comparative simulation study on 3 large-scale facade testing methods, namely, the SP Fire 105, BS 8414-1, and the ISO 13785-2 methods, is presented. Generally good correspondence between simulations and experimental data has been found, provided that thermal properties of the facade material and heat release rates are known; however, the correspondence deviates in close proximity of the fire source. Furthermore, a statistical ensemble for evaluating the effects stemming from uncertainty in input data is used. Here, it was found using this statistical ensemble that the variability was smaller in the ISO 13785-2 compared to the BS 8414-1 method. The heat release rates (HRR) used in the simulations were adopted from measurements except for the ISO method where the information in the standard was used to approximate the HRR. A quantitative similarity between the HRR in the ISO method and the British method was found.

KEYWORDS

fire, facade test, modeling, fire exposure, FDS

1 | INTRODUCTION

External fire spread in buildings has been assessed for a long time using number of different facade fire-test methods.[1-8] The test methods have been proposed to evaluate the fire performance of different wall claddings, insulations, and geometrical considerations.[1,2] The situation today is that a large number of different tests are used for verification and classification of facade systems, ranging from small-scale tests to full-scale tests.[1] Since each country has their own building regulation, there is a large spread in the requirements and on how to show the performance of the facade system.[3]

There are many factors that can influence the effective fire exposure in a test method, and in facade testing, also the surrounding environment is sometimes of great importance. Experimental results show that the effective fire exposure to the facade may vary in SP Fire 105,[9] BS 8414-1,[10] and ISO 13785-2[11] test methods depending on environmental and geometrical factors. All 3 methods define an amount of fuel to be used, eg, in BS 8414-1 and ISO 13785-2, a volume of wood, and in SP Fire 105, a volume of heptane, and the geometry of the combustion chamber. The SP Fire 105 method simulates a 3-story apartment building, height 6.7 m, width 4 m, and depth 1.6 m, shown in Figure 1A, and the BS 8414-1 consists of a main test wall of at least 2.6 m wide and 6.0 m above the fire compartment and a return wall of minimum width of 1.5 m and the same height shown in Figure 1B. The ISO 13785-2 method consists of a main wall that extends at least 4.0 m above the fire room and is at minimum 3.0 m wide and a return wall of the same height that is 1.2 m in width, displayed in Figure 1C. The experimental setup is intended for determining the fire behavior of external wall assemblies and facade claddings. It is thus not possible to actively control (regulate) the heat exposure to the facade surface during a test, and it may differ from test to test because of factors such as air movements around the combustion chamber and geometry of the test specimens. Although in the ISO 13785-2, it is specified that the ventilation conditions can be changed during the calibration test; however, during testing, this should be fixed and not altered. In the SP Fire 105 method, the influence from geometry of the test specimen is important if the boundary of the defined room fire is set as the lower front edge of the facade system. In case of a boundary along the inner edge of the facade system, the thickness is a natural effective parameter for changing the fire exposure of the vertical surface. During testing, falling down of parts and the occurrence of burning droplets is recorded. After fire exposure, the construction, typically a combustible inner core protected by plaster, is cut into pieces to assess the internal fire spread in the core.

A large-scale facade test method is quite complex, and there are many different factors that can affect its repeatability and reproducibility. When wood cribs or liquid pool fires are used, an uncontrolled variability is introduced. The thickness of the test specimen will affect

 Copyright © 2017 John Wiley & Sons, Ltd.

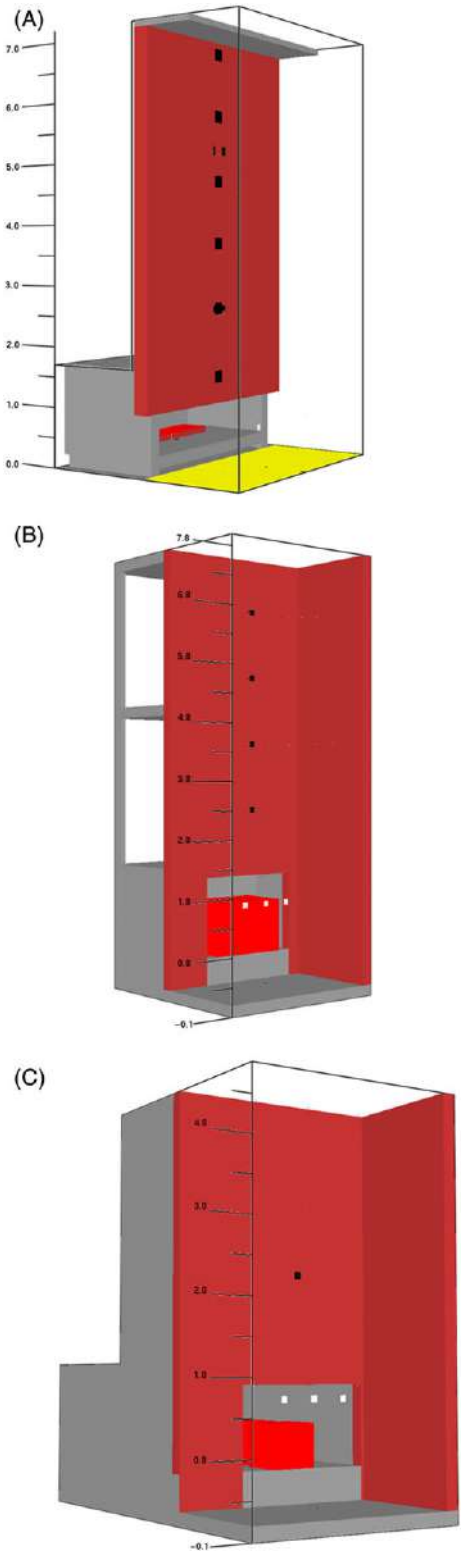


FIGURE 1 The geometries of the experimental methods according to the standards SP Fire 105 (top)[9] with dimensions 6.7 × 4.0 m (height × width), BS 8414-1 (middle) with dimensions 8.0 × 2.6 m and 1.5 m for the return wall[10] and ISO 13785-2 (bottom) with dimensions 5.7 × 3.0 m and 1.2 m for the return wall[11] used in the models. The square objects are plate thermometers where black and white color indicates the front and back of the plate thermometer, respectively [Colour figure can be viewed at wileyonlinelibrary.com]

the exposure since energy will be absorbed by the boundaries before the fire reaches the facade surface, and the dynamical flow of hot gases may change and thus change the heat transfer to the facade. This is because the test system is built on the outside of the rig making the distance from the fire source to the target surface longer for thick systems. Air movements around the test setup (the wind) may also have a significant impact on the test.

The Swedish test method SP Fire 105 was originally developed in the middle of the 1980 ties as a part of a larger study, which included burning of 14 facades with a fully developed fire in a room as a heat source.[3] The fire exposure was calibrated in the SP Fire 105 test to correspond to the exposure measured during the larger tests including a real room fire. In the large reference tests, the fire load density was 110 MJ/m^2 of total surface area of the enclosure. The enclosure dimensions were 4 × 2.2 × 2.6 m^3 with an opening factor of 0.06 m$^{1/2}$. During the tests, approximately 50% of the fuel was estimated to burn outside the chamber. Moreover, similar combustion dynamics is found in the simulations of the SP Fire 105. This excess fuel factor is dependent on the geometry of the enclosure as well as on fuel characteristics such as composition and geometry. In the simulations, the excess fuel factor is estimated by the amount of oxygen flowing in and out of the fire compartment in combination with the fuel-burning rate. The fire source in the SP Fire 105 test is 60 L of heptane burning in trays with attached flame suppressors.

With the help of numerical modeling, it is possible to perform extensive parameter studies and thus determine which parameters, with a natural variation, have an important effect on the robustness of the test method. The use of simulations may also reduce the amount of large-scale development testing, which is inhibited by large costs. Using numerical modeling, within the Fire Dynamics Simulator v 6[12] paradigm, the same trends as found in experiments could be seen.[13-18] In general, good agreement between the experimental data and the numerical model was found when the measured heat release rate (HRR) was used as an input in the simulations. The same correspondence was not found when comparing with additional instrumentation (not included in a standard test) close to the burning chamber where the models gave substantially higher temperatures. Reasons for this are unclear; however, for SP Fire 105, it is possibly a consequence of the shape of the flame suppressing lattice in the fire tray that lead to different local combustion effects compared to burning from a liquid surface not reproduced by using a heat release rate as an input to the simulation. It is interesting to note that a pool fire model not impeded by the flame suppressing lattice has a much faster burning rate and more local combustion effects. The faster burning rate is due to an increase in reradiation to the fuel surface causing a higher evaporation rate of the fuel. We note also that there is consistently a time lag between the simulated results and the measured temperatures. For the wood cribs in BS 8414-1 and ISO 13875-2 that are used as fire sources, possibly similar effects are found because of the fact that a specified HRR is given. There can be several reasons for this time lag, such as measurement of the heat release rate performed far from the fire source and inaccuracies in the precise initial time for the beginning of combustion. In combination, a difference in thermal inertia of

10991018, 2018, 5, Downloaded from https://onlinelibrary.wiley.com/doi/10.1002/fam.2485 by Natl And University Lib In Zagreb, Wiley Online Library on [26/01/2026]. See the Terms and Conditions (https://onlinelibrary.wiley.com/terms-and-conditions) on Wiley Online Library for rules of use; OA articles are governed by the applicable Creative Commons License

the experimental setup compared to the numerical one can occur. Moreover, it can be stemming from modeling choices with a lower fraction of radiative heat transfer.

2 | THE NUMERICAL WORK

The numerical work was performed using FDS version 6.2.0. In the FDS software, the Navier-Stokes equations in the limit of low-speed, thermally driven flow with an emphasis on smoke and heat transport from fires are solved. Historically, in FDS 5, the algorithm used was an explicit predictor-corrector scheme that is a second-order accurate in space and time where turbulence was treated by means of Large Eddy Simulation in the Smagorinsky form, which now has been changed to the Deardorff model in FDS 6.[12] It takes into account heat transfer conditions at walls (1D heat equation solved in solids) and ventilation conditions. The heat transfer by radiation is included in the model via the solution of the radiation transport equation for a gray gas. The equation is solved using a finite volume technique for convective transport; thus, the name given to it is the finite volume method. When using 100 discrete radiation angles, the finite volume solver requires about 20% of the total CPU time of a calculation, a relatively modest cost given the complexity of radiation heat transfer.

In the FDS calculation, a thermal model for plate thermometers was included. The plate thermometer originally developed for controlling the heat exposure in fire resistance furnaces and has also been proven to be a robust alternative to heat flux gauges during fire conditions. The plate thermometer is a physical object measuring an effective temperature that consists of a stainless steel plate (Inconel 600 of size 100 × 100 × 0.7 mm) with a 10-mm-thick insulation pad on the backside. Because of its construction, it will have a finite response time that also has to be taken into account in the modeling, ie, a thermal model for the plate thermometer is needed. In the numerical, we have implemented a physical object with the same dimensions as the experimental counterpart. The thermal material data of the Inconel were taken from the manufacturer's data sheet while the insulation material was characterized by the transient plane source method at SP.[19,20] The emissivity of the steel plate was set to 0.8, which is based on absorptivity measurements.

To validate the model in FDS, a comparison of the step response time was made using a 35-kW/m^2 heat exposure in the cone calorimeter, which yielded a very good agreement.[13] Furthermore, in 3 different models, namely, of the test methods SP Fire 105, BS 8414-1, and ISO 13785-1, the fire room is modeled using Siporex concrete material with density of 500 kg/m^3, heat conductivity of 0.15 W/mK, and specific heat of 1000 J/kg K (indicated by the gray material surrounding the fire room in Figure 1.). To assess the grid sensitivity, a grid resolution study was performed in Jansson and Anderson[13] where it was concluded that a cubic grid of 5 × 5 × 5 cm is suitable for the SP Fire 105 model.

In the model, the wind is imposed as a boundary condition using atmospheric ramp condition, p. 125 in McGrattan et al.[12] In the present work, we report on numerical experiments performed for comparisons with ISO 13785-2, in addition to the BS 8414-1 and SP FIRE 105 methods where we have implemented additional plate thermometers, which are not prescribed in the test methods. In particular, one plate thermometer in front of the fire source and one along the facade have been added, to assess the thermal loads from the fire source and the exposure to the facade specimen, respectively. Of particular interest is the central plate thermometer placed 0.5 m from the fire room (illustrated by a white square in front of the fire room) and a plate thermometer placed flush on the surface of the facade (illustrated by a black square in the first fictitious window of the SP Fire 105 and the corresponding plates in BS 8414-1 and ISO 13785-2) as shown in Figure 1. There are a few particular differences between the methods such that ISO 13785-2 and BS 8414-1 can be used outside and that a return wall is included; see Figure 1. It has been recognized that the wind may have a significant effect on the test, influencing the combustion rate as well as specific results on measurements that may affect the outcome of the test. One important factor determining the exposure on the facade is the HRR of the fire source. In these 3 models, we have used the HRR as presented in Figure 2. Note that the total energy used in the fire source in both BS 8414-1 and ISO 13785-2 is significantly higher than that contained in the 60 liters of heptane used in the SP Fire 105. In Table 1, Figure 2 is further analyzed. The total energy during the first 15 minutes of respective test is also indicated in Table 1. Because the total energy in the methods BS 8414-1 and ISO 785-2 are higher and at the same time the opening to the fire room less wide in comparison to the SP Fire 105 and thus the exposures in those methods are elevated and more localized. One possible complication in comparing results between different methods is the geometrical differences in the size of the opening and the location of the fire room. In this work, we evaluate the fire exposure by plate thermometers placed at the same distance from the lintel of the fire room.

3 | DETERMINISTIC SAMPLING

Because of the lack of knowledge of the precise details of the system, seemingly random behavior can be governed by deterministic, although nonlinear, models. Thus, in such systems, small variations may have a significant change in the outcome. Most of the calculations

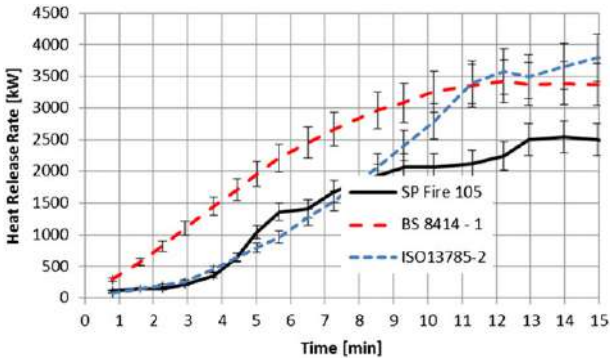


FIGURE 2 The heat release rate (HRR) used in the simulations including the assumed uncertainty of ±10%.[5] The HRR for SP Fire 105 is adopted from measurements in Babrauskas[5] and in the case of BS 8414-1 from measurements presented in Anderson and Jansson.[14] The HRR used in ISO is synthetically constructed and calibrated using the information from the standard[11] [Colour figure can be viewed at wileyonlinelibrary.com]

10991018, 2018, 5, Downloaded from https://onlinelibrary.wiley.com/doi/10.1002/fam.2485 by Natl And University Lib In Zagreb, Wiley Online Library on [26/01/2026]. See the Terms and Conditions (https://onlinelibrary.wiley.com/terms-and-conditions) on Wiley Online Library for rules of use; OA articles are governed by the applicable Creative Commons License

TABLE 1 Energy prescribed in simulations, analysis of Figure 2

Test Method	Total Energy, MJ (Energy released during first 15 min [MJ])	Total Energy Per Meter Width of Opening, MJ/m (Energy released per meter during first 15 min [MJ/m])
BS 8414-1	2163	1082
ISO 13785-2	1715	858
SP Fire 105	1334	445

both numerical and analytical are often performed with very little thought given to these uncertainties, and thus, designs are often based on potentially inaccurate information. Moreover, modeling is often performed in stages by different numerical or analytical tools where the uncertainties may propagate through the system without much control.[17,18] It is usually a very difficult task to objectively establish the confidence levels in numerical predictions. Uncertainty Quantification (UQ) is the science of quantitative characterization and reduction of uncertainties in numerical studies and real world experimentation. The UQ aims at determining how likely certain outcomes are if some aspects of the system are unknown. Deterministic Sampling (DS)[21,22] is a relatively new method used for UQ and is used in this paper to offer an efficient alternative. The method is based on the idea that a continuous probability density function can be replaced by an ensemble of discrete deterministic samples, provided that the 2 representations have the same statistical moments. This method is related to the fractional factorial design method in that simulations using the maximum and minimum values of the variability are utilized in the simulations.

Quality assurance in CFD simulations[23] is of great importance to provide reliable simulations and with the possibility of validation against experimental results. In this section, we shortly summarize the theoretical background that is the basis for the explicit choices of ensembles used in this work. We will construct an example where 5 parameters are modeled uncertain since this is the needed input to the numerical model; however, to reduce to computational time, we will reduce the study to include only a few particular parameters of interest. In the absence of correlations, the ensemble of m samples are given by

$$\Sigma = \langle\theta\rangle \otimes 1^{1\times m} + \operatorname{diag}\left(\langle\theta\rangle \circ \operatorname{std}\left(\frac{\theta}{\langle\theta\rangle}\right)\right)\cdot\widehat{V},$$

where $1^{1\times m}$ denotes a row vector of m "ones," $\otimes$ outer product, $\circ$ element-wise multiplication, and diag(X) is the diagonal matrix with the vector X on its diagonal. Here std is the standard deviation. The excitation matrix $\widehat{V}$ contains all variations; each column describes one "normalized" model sample variation from its mean. In Table 2, the variations in 5 of the main parameters are presented. There are thus, n = 5 parameters that need to be modeled uncertain. For instance, the standard (STD) ensemble can be used:

$$\widehat{V}_{STD} = \sqrt{n}\cdot(I_{n\times n} \;\; -I_{n\times n}) = \begin{pmatrix} \sqrt{5} & 0 & 0 & 0 & 0 & -\sqrt{5} & 0 & 0 & 0 & 0 \\ 0 & \sqrt{5} & 0 & 0 & 0 & 0 & -\sqrt{5} & 0 & 0 & 0 \\ 0 & 0 & \sqrt{5} & 0 & 0 & 0 & 0 & -\sqrt{5} & 0 & 0 \\ 0 & 0 & 0 & \sqrt{5} & 0 & 0 & 0 & 0 & -\sqrt{5} & 0 \\ 0 & 0 & 0 & 0 & \sqrt{5} & 0 & 0 & 0 & 0 & -\sqrt{5} \end{pmatrix}.$$

The most computationally efficient way of investigating the outcome of variations in certain parameters is however to vary all parameters at the same time. One such example is the binary (BIN) ensemble created by permutations of ±1,

$$\widehat{V}_{BIN} = \begin{pmatrix} +1 & -1 & +1 & -1 & +1 & -1 \\ +1 & +1 & -1 & -1 & +1 & +1 \\ -1 & +1 & +1 & -1 & -1 & +1 \\ +1 & +1 & +1 & +1 & -1 & -1 \\ -1 & -1 & +1 & +1 & +1 & +1 \end{pmatrix}.$$

Note: The maximum variation of the standard ensemble is $\sqrt{5}$, while it is only 1 for the binary. By varying all parameters in all samples of the binary ensemble, its maximum variation is minimized. The risk of "saturating" the model is thereby minimal with the BIN ensemble. The standard ensemble is easily generalized, but the binary ensemble has a more complex construction. Calculating the *model ensemble* by evaluating the model H for every sample (column) of Σ produces the row vector $H(\Sigma)$ of m results. The expected result is given by

$$\langle H\rangle = \langle H(\Sigma)\rangle = H(\Sigma)\cdot(1/m)^{m\times 1}.$$

The results from the computational work $H(\langle\theta\rangle)$ will be compared to experimental results. If the difference is large, nonlinear effects are significant. If the difference is small, it is likely, but not sure, that the model can be approximated to be linear.

The variance of the model result is given by

$$\operatorname{var}(H) = \left\langle \left(H(\Sigma) - \langle H(\Sigma)\rangle\right)^2 \right\rangle = \left(H(\Sigma) - \langle H(\Sigma)\rangle\cdot 1^{1\times m}\right)^2\cdot(1/m)^{m\times 1}.$$

Assuming a coverage factor $k = 2$ for also the result, the modeling uncertainty will be,

$$\operatorname{unc}(\mathrm{H}) = 2\sqrt{\operatorname{var}(H)}.$$

In summary, the confidence interval of the modeling result is given by

$$\left[\langle \mathrm{H}\rangle - 2\sqrt{\operatorname{var}(H)}, \langle \mathrm{H}\rangle + 2\sqrt{\operatorname{var}(H)}\right].$$

The methodology will now be applied to assess uncertainties in a CFD model of the BS8414-1 and ISO 13785-2 facade fire

TABLE 2 The variations used in the uncertainty quantification in all 3 models

Parameter	Mean Value	Variation
Thermal conductivity k, W/(m K)	0.242	±30%
Density ρ, kg/m^3	975	±30%
Specific heat capacity c_p, J/(kg K)	1000	±30%
Heat release rate, kW	See Figure 2	±10%
Wind U_0, m/s	0.5	±0.5 m/s

Note that the variations in the thermal material data only reflect a change of material and not actual measurements of the thermal data.

10991018, 2018, 5, Downloaded from https://onlinelibrary.wiley.com/doi/10.1002/fam.2485 by Natl And University Lib In Zagreb, Wiley Online Library on [26/01/2026]. See the Terms and Conditions (https://onlinelibrary.wiley.com/terms-and-conditions) on Wiley Online Library for rules of use; OA articles are governed by the applicable Creative Commons License

testing methods. A similar exercise was previously performed for the SP Fire 105.[16]

4 | ESTIMATING UNCERTAINTIES IN A CFD MODEL

In this section, we will evaluate and compare the numerical models developed for SP Fire 105, BS 8414-1, and ISO 13785 facilities. In general, we have previously found good agreement and qualitatively the same behavior in comparing simulation results to experimental data, see previous studies[13-16]; however, there are lot of uncertainties accompanying the input data of simulations. Thus, we have to take these uncertainties into account in the models. In this work, 5 parameters used in the models of the BS 8414-1 and ISO 13785-2 facade fire tests have been introduced, and results obtained are compared with previous simulations. A similar result was found for the BS 8414-1 and ISO 13785-2 in the present study. Note that in this work, we will only discuss uncertainties stemming from uncertainties in the input data, and not from grid resolution although a preliminary sensitivity study was performed. The parameters with assumed uncertainties are summarized in Table 2 below; note that all uncertainties are assumed and are only used in this model to investigate how they propagate through a nonlinear model. The general problem of uncertainty quantification in CFD models is usually limited by long simulation times, and thus, only a few parameters are feasible to investigate. However, by using deterministic sampling allows for investigations of variations in significantly more parameters. Adequate uncertainty quantification with a low number of simulations is thus now within reach. Here, we can estimate the variance in the output with only 6 simulations where 5 parameters are to be modeled uncertain. Although the assumed variations in the material parameters are larger than can be assumed from measurements and this variability is used to assess the dependence of different material properties of the facade on the computed results. The parameters in Table 2 are given with maximum deviation around the mean value. Note that the mean values of the material data are taken from typical values of fiber reinforced polymer material.

4.1 | Modeling of SP fire 105

Before presenting the evaluations of the uncertainty in the model, we enlighten the reader on the comparison between numerical results and experimental measurements for the SP Fire 105. The results presented here are a reproduction of the results presented in Anderson et al[15,16] and are shown to simplify the comparative work. The thermal data for the material are taken as the mean values in Table 2 and the HRR is shown in Figure 2. The resulting temperatures shown in this paper are evaluated by a plate thermometer modeled as a physical object as was done previously in other studies.[13,14]

In Figures 3 and 4, we have gauged the fire source by PTs 0.5 m from the fire room and one PT pointing outwards 2.1 m above the upper edge of the fire room (beside the heat flux meter in the fictitious window). The fictitious windows are just indentations in the facade specimen. These measurements are in addition to the standardized

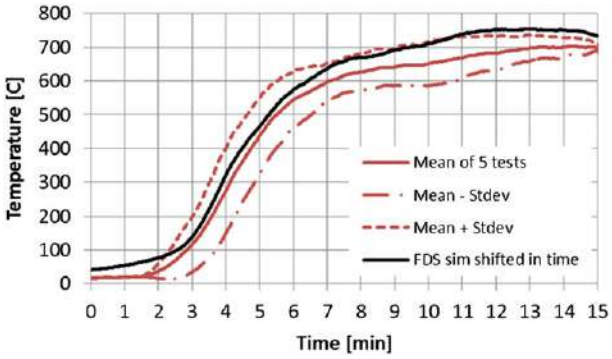


FIGURE 3 The resulting temperatures from the PT in front of the facade, 0.5 m from the fire room [Colour figure can be viewed at wileyonlinelibrary.com]

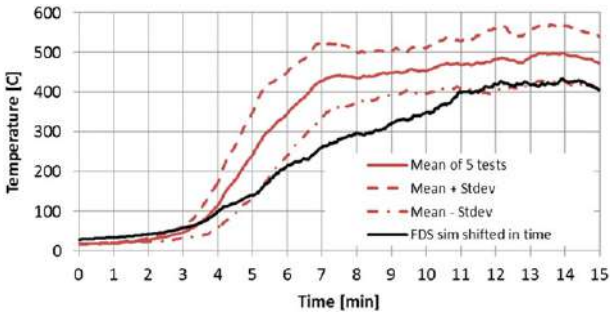


FIGURE 4 The resulting temperatures from the PT in the first fictitious window, 2.1 m above the fire room [Colour figure can be viewed at wileyonlinelibrary.com]

measurements specified in the method. The experimental data are taken from tests with 3 different wood materials with facade systems containing fire retardants, one brick wall with combustible insulation and one directly exposed insulation of phenolic resin. The data from the 5 tests are used to compute mean value and standard deviation and then compared to the results from the simulation with facade properties indicated in Table 2. We have adjusted the time (30 s) for the simulation to roughly match the exposure in Figure 3 finding a quite good qualitative and quantitative agreement mostly within one standard deviation. We have approximately the same amount of uncertainty around 3% in the computed temperatures determined by evaluating the standard deviation of the time series, ie, the measured temperatures are roughly within one standard deviation of the computed temperature. In Figure 4, the exposure on the facade is estimated by a PT where we find that the temperatures in the simulation are significantly lower than those in the test; however, there is a significant contribution to the HRR from the wood and phenolic resin facade systems yielding increased measured temperatures. In the simulations, this has been accounted for only as an increase in the total HRR released by the burner and thus additional combustion on the facade is neglected.

Naturally, the thickness of the test specimen will affect the exposure since energy will be lost to the surroundings, and the underside of the facade system before the fire reaches the vertical facade surface when we define the fire load at the inner edge of the underside of the facade system. Moreover, a specimen that significantly stretches

10991018, 2018, 5, Downloaded from https://onlinelibrary.wiley.com/doi/10.1002/fam.2485 by Natl And University Lib In Zagreb, Wiley Online Library on [26/01/2026]. See the Terms and Conditions (https://onlinelibrary.wiley.com/terms-and-conditions) on Wiley Online Library for rules of use; OA articles are governed by the applicable Creative Commons License

out from the facade rig may change the flow pattern of hot gases out of the fire room and thus change the local fire dynamics and the heat transfer, see Figure 5.

In Figures 6 and 7, the simulated temperatures are shown for a regular facade (100 mm) and a thicker facade (330 mm) system. The computed temperatures are evaluated in front of the facade 0.5 m from the fire room and at the midpoint the length of the fire room opening (pointing towards the fire source) and 2.1 m above the opening of the fire room in the middle of the first fictitious window below the heat flux gauge included in the standard testing (pointing outwards towards the plume), see Figure 1. The heat flux gauge is a common water-cooled Schmidt-Boelter device.

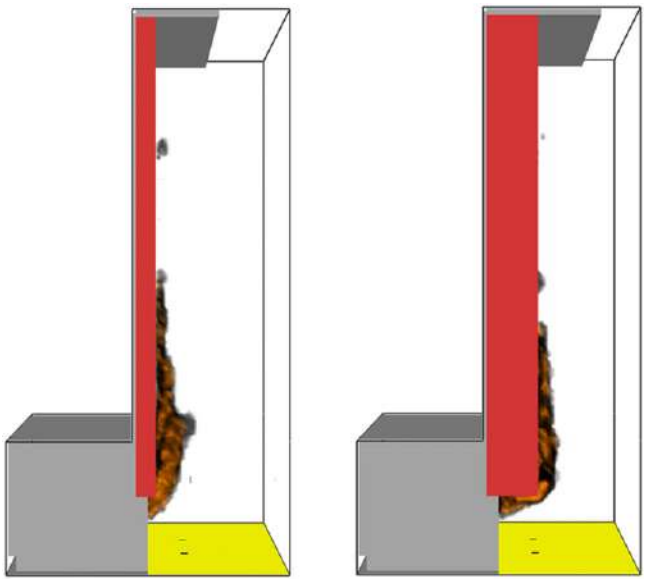


FIGURE 5 Geometrical factor in test methods illustrated in an fire dynamics simulator model [Colour figure can be viewed at wileyonlinelibrary.com]

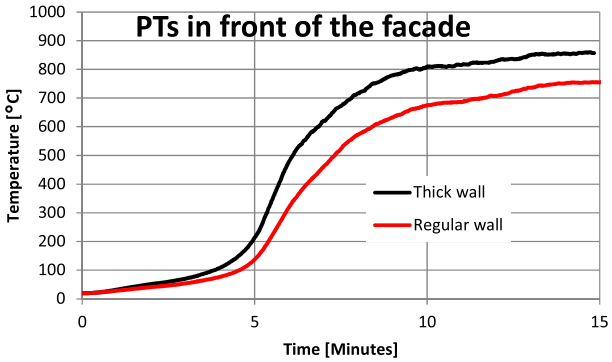


FIGURE 6 Temperature computed by the plate thermometer model in front of the facade in SP Fire 105, as shown in Figure 1 [Colour figure can be viewed at wileyonlinelibrary.com]

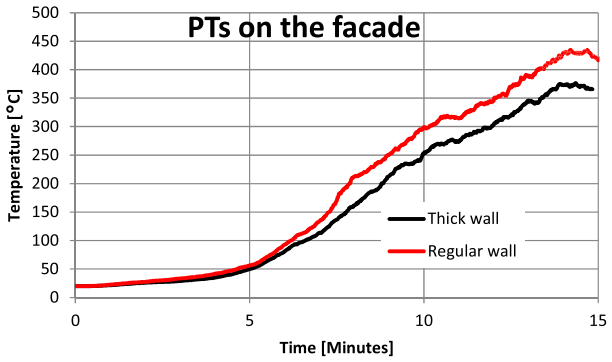


FIGURE 7 Temperature computed by the plate thermometer model on the facade in SP Fire 105, as shown in Figure 1 [Colour figure can be viewed at wileyonlinelibrary.com]

We find that the temperature in front of the facade is increased with a thicker facade specimen protruding further out from the regular holding rig. Here, it is interesting to note that the reverse behavior is found for the temperature measured by the plate thermometers on the wall, as shown in Figures 6 and 7. This shows the same qualitative and quantitative behavior as found in the experimental comparison performed in Anderson et al[15] where an increased temperature in front of the facade whereas a decreased temperature on the facade 2.1 m above the fire room is observed. The dynamics of the plume and the heat transfer into the facade specimen is changed for the thicker specimen seemingly leading to this difference. Because of the extension of the facade, the flows direct the hot gases slightly more away from the fire room closer to the PT in front of the facade and at the same time limit the exposure to the main wall occupied by the specimen. This leads to an increased temperature in front of the facade.

4.2 | Modeling of BS 8414-1

Here, analogous modeling of the BS 8414-1 is presented, where time slices of the gas temperatures of the simulation are shown in Figure 8. The temperature plot shows significant mixing of colder air and hotter gases from the fire. We have performed simulations according to the deterministic sampling scheme presented in section dedicated to deterministic sampling using the variations from Table 2 and the HRR presented in Figure 2. In a similar manner, the temperature obtained by a plate thermometer in front of the fire source is shown in Figure 9. The temperature was also measured with a plate thermometer located 1.25 m above the top edge of the fuel chamber as displayed in Figure 10. This plate thermometer was placed 10 cm from the facade surface and pointing outwards, ie, it measures the incident heat exposure to the facade. Note that the placement of the measurements is approximately at the same location as in the SP Fire 105 considering the height above ground; however, only results for the thin facade specimen are shown. The red dashed lines represent the mean value ± one standard deviation.

In a previous study, a good correspondence between simulations and the experimental work was found; however, in that comparison, the wind effect was neglected and thus a variability that existed in the experimental result was lacking.[15,16] In this work, we have included a constant wind of 0.5 ± 0.5 m/s, and thus in the simulation, we have used 0 and 1 m/s; however, in the experimental situation, the wind varied quite a lot. The resulting temperatures in Figures 9 and 10 follow the evolution of the HRR, and it is evident that the wind introduces a significant deviation in the temperatures both in front of the fire source and on the facade. The artificial wind in the model move the plume to the side; thus, the hot gases are further from the PT in front of the facade as well as the PT on the facade leading to reduced temperatures.

10991018, 2018, 5, Downloaded from https://onlinelibrary.wiley.com/doi/10.1002/fam.2485 by Natl And University Lib In Zagreb, Wiley Online Library on [26/01/2026]. See the Terms and Conditions (https://onlinelibrary.wiley.com/terms-and-conditions) on Wiley Online Library for rules of use; OA articles are governed by the applicable Creative Commons License

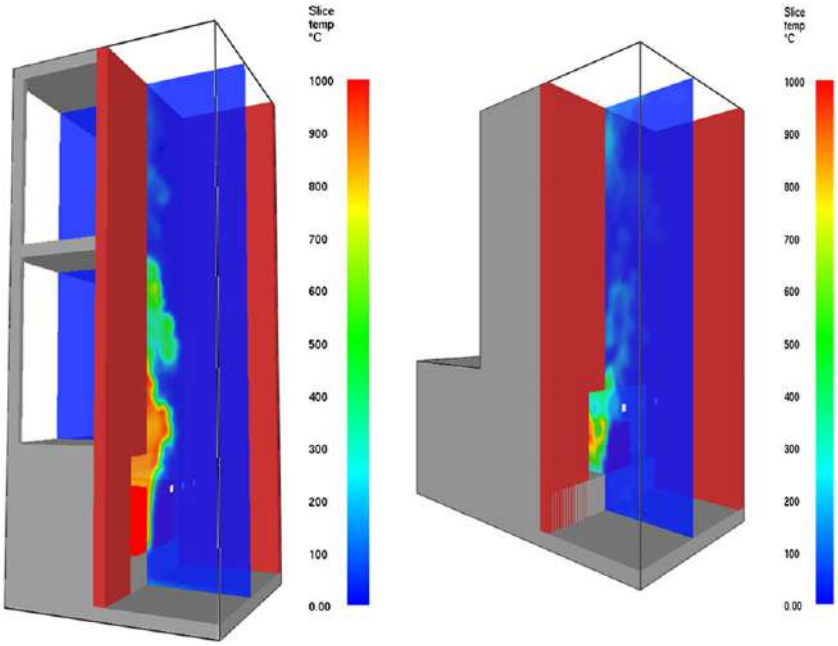


FIGURE 8 Representation of the simulation models in FDS of the BS 8414-1 (left) and the ISO 13785-1 (right) fire testing methods. The time slices of the temperatures are taken at 600 seconds into the simulation [Colour figure can be viewed at wileyonlinelibrary.com]

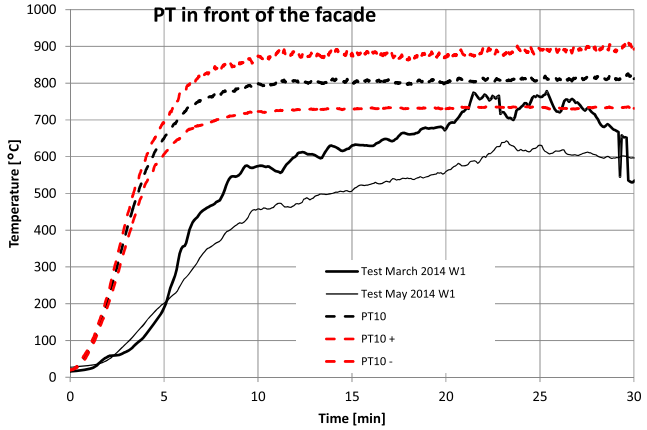


FIGURE 9 Temperature computed by the plate thermometer model in front of the BS 8414-1 facade, as indicated in Figure 1. Here, PT 10 ± refers to ± one standard deviation [Colour figure can be viewed at wileyonlinelibrary.com]

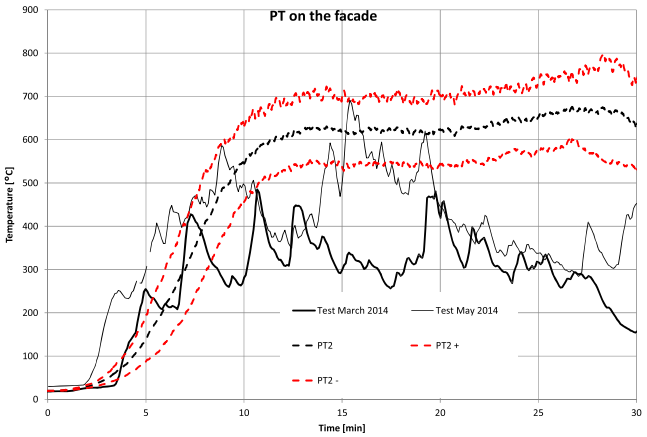


FIGURE 10 Temperature computed by the plate thermometer model on the BS 8414-1 facade, as indicated by Figure 1. Here, PT 2 ± refers to ± one standard deviation [Colour figure can be viewed at wileyonlinelibrary.com]

4.3 | Modeling of ISO 13785-2

Similar to the cases of SP Fire 105 and the BS 8414-1, we performed a computational study of the ISO 13785-2 test method using the same instrumentation for evaluation; however, only results for the thin facade specimen are shown. We used the HRR presented in Figure 2, which is numerically calibrated by the information given in the standard[11] unlike the other 2 cases where the HRR were adopted from measurements. Note that, during full fire exposure in the calibration test the front face of the facade shall be subjected to a total heat flux of 55 ± 5 kW/m^2 measured by the 3 heat flux meters placed directly above and along a line parallel to the horizontal centerline of the fire room opening (see Figure 1). The total heat flux at 1.6 m above the window opening shall be 35 ± 5 kW/m^2; however, it seems difficult to fulfill both requirements of heat flux. In the simulation, we have calibrated the heat flux at the top heat flux gauges to be just below 40 kW/m^2; on the other hand, this gives a total heat flux at the lower level of almost 80 kW/m^2. If on the other hand, we calibrate the heat flux at the lower level, we find that the measurement at 1.6 m above the window is significantly lower than 30 kW/m^2.

To have a conservative case, we used the HRR giving the higher heat flux values in this work, which is given by the HRR that is given in Figure 2. Note that the peak plateau of the HRR is rather similar to that of the BS 8414-1 case; thus, we expect rather similar results in terms of computed temperatures since we are considering cases with otherwise similar conditions. We note that there is a small plateau in the temperature in Figure 11, corresponding to the small dip in HRR in Figure 2. In Figures 11 and 12, the corresponding temperatures measured by plate thermometers in front of the facade and on the facade at 3.25 m above ground are shown, respectively. The red dashed lines represent the mean value ± one standard deviation of the variations found using the deterministic sampling method. Note that rather modest changes in the HRR used may have significant effect on the plate temperatures.

10991018, 2018, 5, Downloaded from https://onlinelibrary.wiley.com/doi/10.1002/fam.2485 by Natl And University Lib In Zagreb, Wiley Online Library on [26/01/2026]. See the Terms and Conditions (https://onlinelibrary.wiley.com/terms-and-conditions) on Wiley Online Library for rules of use; OA articles are governed by the applicable Creative Commons License

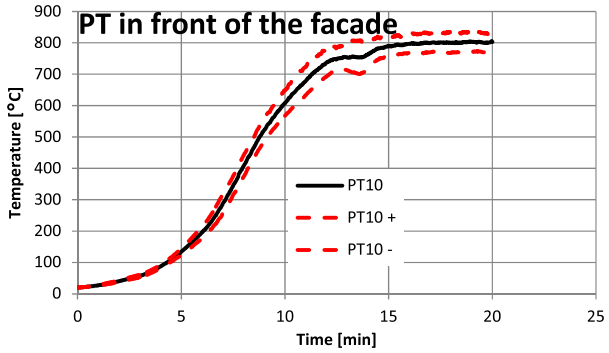


FIGURE 11 Temperature computed by the plate thermometer model in front of the ISO13785-2 facade. Here, PT 10 ± refers to ± one standard deviation [Colour figure can be viewed at wileyonlinelibrary.com]

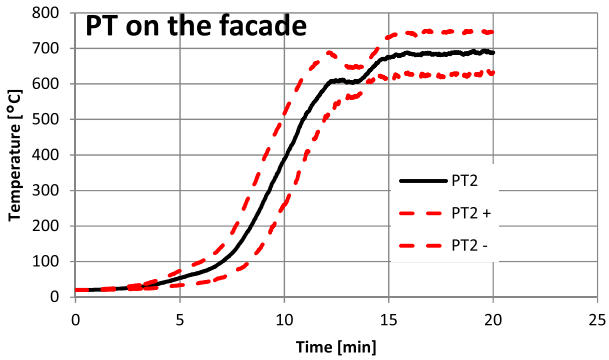


FIGURE 12 Temperature computed by the plate thermometer model on the ISO13785-2 facade. Here, PT 2 ± refers to ± one standard deviation [Colour figure can be viewed at wileyonlinelibrary.com]

Comparing the temperatures found in the BS 8414-1 and ISO 13785-2 models, it is computed that they are quantitatively the same at the plateau where the fire intensity is at maximum. However, because of a slightly faster fire growth in BS 8414-1 model, this maximum is reached earlier in this case. We note that the statistical variation as measured by the standard deviation is smaller for the ISO 13875-2 model compared to the BS 8414-1 model although the same variation in the input parameters are used. Furthermore, it is only around 3% for SP Fire 105 for the plate thermometer data as seen in Anderson et al.[16] It is important to note here that the material in the burning chamber is kept the same in all 3 models and to be that of Siporex.

In Tables 3 and 4, we present a summary of the simulation results in terms of mean value and standard deviation averaged over 1 minute at maximum fire intensity between 14 and 15 minutes. We note that

TABLE 3 Summary of the results in front of the facade in mean values and standard deviations contrasted at the maximum fire intensity averaged over 1 minute between 14 and 15 minutes

Simulation	Mean (Max Fire Intensity), °C	Std (Max Fire Intensity), °C	Std/Mean
SP Fire 105	744	23	0.031
BS 8414-1	806	76	0.094
ISO 13785-2	779	35	0.044

TABLE 4 Summary of the results on the facade in mean values and standard deviations contrasted at the maximum fire intensity averaged over 1 minute between 14 and 15 minutes

Simulation	Mean (Max Fire Intensity), °C	Std (Max Fire Intensity), °C	Std/Mean
SP Fire 105	421	15	0.035
BS 8414-1	624	79	0.127
ISO 13785-2	658	43	0.065

the standard deviation for BS 8414-2 is much larger than for the other 2 methods. One of the reasons here is the difference in flow dynamics since the fire room is very small in comparison to the fire load, which seems to give a different dynamics of the flows along the facade.

5 | DISCUSSIONS AND CONCLUSIONS

We present detailed comparisons between the results from the different numerical models representing the ISO 13785-2, BS 8414-1, and the SP Fire 105 testing methods. The numerical models where evaluated in the same manner by plate thermometer models in front of the fire source 0.5 m away and on the facade 2.1 m above the combustion chamber; thus, the numerical models have been constructed with analogous geometry and instrumentation. There are some differences between the methods, eg, the SP Fire 105 test is performed indoors in a fire-testing hall, and thus, the air movements are kept on a very low level. The method is similar to BS 8141-1 and ISO 13785-2 with respect to size, although SP Fire 105 does not have the lateral return wall as the British and the ISO methods. Another difference is the fuel used. The ISO and the British method use wood while SP Fire 105 used 60-L heptane and the height of the combustion chamber is 710 mm in SP Fire 105 while it is 2000 mm in BS 8141-1. Here, one important simplification in the modeling is assumed, namely, that the contribution to the HRR of additional combustible matter in the facade system is small compared to the fire source (within 10%). To ensure a robust, repeatable, and reproducible test method for facades, there are several issues that must be resolved. The heat exposure on the facade can, for example, be measured with plate thermometers, which is more linked with the thermal exposure of the facade surface compared to conventional thermocouples. This is based on the assumption that plate thermometers measure an effective or representative temperature due to the thermal exposure from a certain direction rather than a thermocouple that is influenced by the hot gases from all sides. A possible solution is to define a heat exposure curve, as in fire resistance testing, and use gas burners that can be regulated instead of using a defined amount of free burning fuel, ie, defining a time-temperature curve for the plate thermometer on the facade specimen. The appropriate level and nature of the fire source has been debated for a long time and is in need of reassessment. In the SP Fire 105, combustion of internal components in the facade system is in practice checked by visual means, and here, it would be much more preferable to use distinct measurements with, eg, some type of thermocouples. To be able to use simulations as a complement to testing during the development phase, the natural variations have to be taken into account in the models. The present work shows deterministic sampling as a powerful

10991018, 2018, 5, Downloaded from https://onlinelibrary.wiley.com/doi/10.1002/fam.2485 by Natl And University Lib In Zagreb, Wiley Online Library on [26/01/2026]. See the Terms and Conditions (https://onlinelibrary.wiley.com/terms-and-conditions) on Wiley Online Library for rules of use; OA articles are governed by the applicable Creative Commons License

and feasible tool to evaluate how uncertainties propagate through nonlinear models. We see that simulations can easily elucidate on effects of variations to current designs or testing methods, which means that it can be used during the development phase. In particular, it would be interested to extend the model to accommodate for combustible materials in the facade system developed by evaluating additional tests and thorough characterization of materials.

ACKNOWLEDGMENTS

The research was supported by the Swedish Fire Research Board (Brandforsk) with grant BF-14-0011.

ORCID

J. Anderson http://orcid.org/0000-0001-7524-0314

REFERENCES

1. Hildebrand C. Façade fire testing, report CIB 14 workshop, Institute fur Baustoffe, Leipzig, April 1988.
2. Ondrus J, Pettersson O. Fire hazards of façades with externally applied additional thermal insulation—full scale experiments, LUTVDG/TVBB-3025 (1986).
3. Ondrus J. Fire hazards of façades with externally applied additional thermal insulation—full scale experiments, LUTVDG/TVBB-3021 (1985).
4. Oleszkiewicz I. Heat transfer from a window fire plume to a building façade, Collected Papers in Heat Transfer, H00526, p. 163–170 (1989).
5. Babrauskas V. Facade fire tests: towards an international test standard. *Fire Technology*. 1996;32:219-230.
6. Abecassis Empis C. Analysis of the compartment fire parameters influencing the heat flux incident on the structural façade, PhD thesis, University of Edinburgh (2010).
7. Strömgren M, Albrektsson J, Johansson A, Almgren E. Comparative analysis of façade regulations in the Nordic countries, MATEC Web of Conferences 9, 01003 (2013).
8. Bytskov G. Numerical simulation of fire performance and test conditions for façade insulation materials, MSc Thesis, Aalto University (2015).
9. SP FIRE 105—Method for fire testing of façade materials, Dnr 171-79-360 Department of Fire Technology, Swedish National Testing and Research Institute.
10. British Standard BS 8414-1:2002, Fire performance of external cladding systems—Part 1: test method for non-loadbearing external cladding systems applied to the face of the building (2002).
11. ISO 13785-2:2002 Reaction-to-fire tests for facades—Part 2: large-scale test. International Organization for Standardization.
12. McGrattan K, McDermott R, Hostikka S, Floyd J. Fire dynamics simulator (version 6)—user's guide. NIST Special Publication 2014.
13. Jansson R, Anderson J. Experimental and numerical investigation of fire dynamics in a facade test rig, Proceedings of Fire Computer Modeling, Santander, p. 247, Spain, 18-19th October 2012.
14. Anderson J, Jansson R. Façade fire tests—measurements and modeling, MATEC Web of Conferences 9, 02003 (2013).
15. Anderson J, Boström L, Jansson R, Milovanović B. Fire dynamics in outdoors façade fire tests: measurement, modeling and repeatability, Proceedings of the Applications of Structural Fire Engineering (ASFE15), 15–16 October, Dubrovnik, Croatia (2015).
16. Anderson J, Boström L, Jansson R, Milovanović B. Uncertainties in facade fire tests—measurement and modeling, The second international seminar for fire safety of façades, Lund 11–13 May 2016.
17. Hostikka S, Bytskov G. Numerical simulations of the ISO 13785-2 façade fire tests, MATEC Web of Conferences 46, 03003 (2016)
18. Drean V, Schillinger R, Auguin G. Fire exposed facades: numerical modelling of the LEPIR2 testing facility, MATEC Web of Conferences 46, 03001 (2016).
19. Hermansson K. Quality assurance and the simulation of fires—a practical application for automated validation of user-generated input data for FDS, Thesis Report 5501 Lund University (2015).
20. Häggkvist A. The plate thermometer as a mean of calculation incident heat radiation, Master thesis, 2009:183 CIV, Luleå University (2009)
21. Hessling JP. Deterministic sampling of propagating model covariance. *SIAM/ASA J Uncertainty Quantification*. 2013;1:297-318.
22. Quality Management in Engineering Simulation, A Primer for NAFEMS QSS, NAFEMS 2014.
23. Guide for the verification and validation of computational fluid dynamics simulations (AIAA G-077-1998(2002)).

How to cite this article: Anderson J, Boström L, Jansson McNamee R, Milovanović B. Modeling of fire exposure in facade fire testing. *Fire and Materials*. 2018;42:475–483. https://doi.org/10.1002/fam.2485

10991018, 2018, 5, Downloaded from https://onlinelibrary.wiley.com/doi/10.1002/fam.2485 by Natl And University Lib In Zagreb, Wiley Online Library on [26/01/2026]. See the Terms and Conditions (https://onlinelibrary.wiley.com/terms-and-conditions) on Wiley Online Library for rules of use; OA articles are governed by the applicable Creative Commons License